Journal of Chromatography A, 1218 (2011) 1340–1346

Contents lists available at ScienceDirect

Journal of Chromatography A

journal homepage: www.elsevier.com/locate/chroma

Recognition characteristics of molecularly imprinted microspheres for triazine herbicides using hydrogen-bond array strategy and their analytical applications for corn and soil samples

Suqin Wu, Zhiguang Xu, Qionghui Yuan, Youwen Tang*, Xiongjun Zuo, Jiaping Lai

School of Chemistry & Environment, South China Normal University, Guangzhou 510006, China

ARTICLE INFO

Article history:
Received 28 August 2010
Received in revised form
29 December 2010
Accepted 5 January 2011
Available online 11 January 2011

Keywords:
Molecularly imprinted microspheres
Hydrogen-bond array
Homogeneous interaction
Simetryne
Precipitation polymerization

ABSTRACT

The homogeneous molecularly imprinted microspheres (MIMs) based on a biologically inspired hydrogen-bond array were prepared using allobarbital as the novel functional monomer and divinylbenzene as the cross-linker. The host–guest binding characteristics were examined by molecular simulation and infrared spectroscopy. The resultant MIMs were evaluated using high performance liquid chromatography and solid-phase extraction. The results obtained demonstrate that the good imprinting effect and the excellent selectivity of MIMs are mainly due to the interaction involving the formation of three-point hydrogen bond between host and guest. The complete baseline separation was obtained for five triazine analogues and a metabolite on the MIM HPLC column. The MIMs were further successfully used as a specific sorbent for selective extraction of simetryne from corn and soil samples by molecularly imprinted solid phase extraction. Detection limits and recoveries were 5.8 μg/kg and 0.14 μg/kg and 87.4–105% and 94.6–101% for simetryne in corn and soil sample, respectively.

1. Introduction

Molecular imprinting is a versatile and easy method for preparing synthetic polymers with predetermined molecular recognition properties [1]. In recent years, molecularly imprinted polymers (MIPs) have been successfully used in solid-phase extractions (SPE) [2,3], chromatographic separations [4–6], as biomimetic sensors [7,8] and mimetic enzyme catalysts [9–11]. A common approach to MIP synthesis involves the association of functional monomers and template molecules prior to polymerization in the presence of cross-linkers. After polymerization and guest molecule (template) is removed, the resultant polymer maintains a structural "memory" of the electronic and geometric nature of the guest molecule, which can be characterized by a variety of techniques.

The local temperature changes during exothermic polymerization reaction might result in nonequilibrium structures and could make the final polymer morphology heterogeneous, with the length scale only slightly larger than the size of the imprinted cavities. This heterogeneity of imprinted matrix affects the specific binding of target molecules [12]. Therefore, better defined and unambiguous host–guest binding modes need to be used to study the binding mechanism of MIPs.

The objective of our work was to develop a molecularly imprinted polymer with a homogenous binding site, suitable for precise investigation of recognition mechanism between host and guest molecules. The MIPs based on three-point hydrogen-bonding motif [13–16] are the ideal candidates; in the past they were usually prepared using ethylene-glycol dimethylacrylate (EGDMA) or tripropyleneglycol diacrylate (TPGDA) as the cross-linker. However, both EGDMA and TPGDA could affect the non-covalent binding of template and functional monomer due to the interactions of their carbonyl group with the amino- or hydroxyl-groups of the template. To eliminate those effects as much as possible in the present study, divinylbenzene (DVB) was employed as the cross-linker to prepare molecularly imprinted microspheres (MIMs) via precipitation polymerization. MIMs allow fast transmission of reaction heat between resultant polymer and medium, resulting in a more homogenous MIP structure.

Recently, increasing environmental awareness has encouraged the efforts to put into investigation of the effect of the residues and metabolites of triazine herbicides on the environment [17–24], particularly the simulation and study of the interactions of proteins and enzymes with triazine herbicides [25]. In this paper, simetryne (SMT), a typical triazine herbicide, was selected as the template molecule. To satisfy the condition of formation of hydrogen-bond array between template and functional monomer, the biological analogue allobarbital (ABA) with a cyclic amide configuration was used as a novel functional monomer. The hydrogen-bond array is easily formed between SMT and ABA (Fig. 1). Furthermore, there are

* Corresponding author. Tel.: +86 20 39310369; fax: +86 20 39310187.
E-mail address: tanglab@scnu.edu.cn (Y. Tang).

0021-9673/$ – see front matter © 2011 Elsevier B.V. All rights reserved.
doi:10.1016/j.chroma.2011.01.008

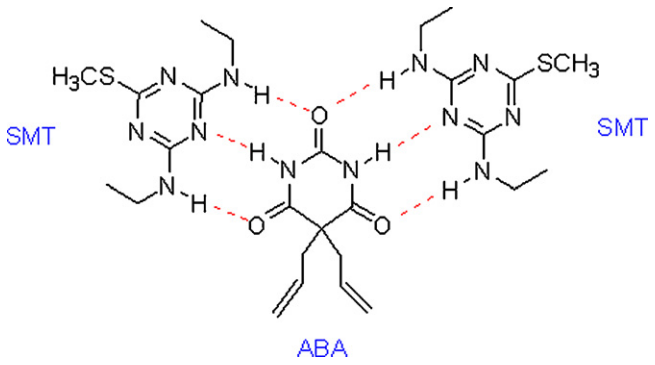

Fig. 1. The interaction of SMT–ABA–SMT via a hydrogen-bond array.

a lot of analogues of SMT which can be used in the investigation of the MIMs' molecular recognition mechanism.

Hereby, this paper mainly focuses on designing and constructing homogeneous MIMs using ABA and DVB as the function monomer and cross-linker, and then investigating the homogeneous interaction between host and guest molecules. Molecular simulation and infrared spectroscopy (IR) were used to probe the binding characteristics of pre- and post-polymerization. The molecular recognition mechanism of the MIMs was further investigated by taking advantage of the HPLC method. This study also attempted to apply the MIMs as a specific sorbent in selective extraction of SMT and its analogues from soil and corn samples.

2. Materials and methods

2.1. Reagents and chemicals

SMT, simazine, atrazine, terbutylazine, propazine, cyanazine, ametryn, and terbutryn (Fig. 2) were kindly provided by Bingzhou Pesticide Plant (Shandong, China). Metribuzin, 4,6-diamino-2-hydroxy-1,3,5-triazine (DAHT), alkyl bromide, barbituric acid, divinylbenzene (DVB), 2,2′-azobisisobutyronitrile (AIBN) were obtained from Alfa Aesar (Tianjin, China). The HPLC grade organic solvents: toluene, acetonitrile, acetic acid and methanol were purchased from Kermel (Tianjin, China).

IR and NMR spectra were obtained using a Bruker (Ettlingen, German) EQUINOX-55 FT-IR instrument and a Varian (Palo Alto, CA, USA) 400 MHz NMR Systems, respectively. Average pore diameter and surface area of the sorbents were measured by nitrogen adsorption with an ASAP2020 Surface Area and Porosity Analyzer of the Micromeritics Company (Norcross City, GA, USA). The SEM micrographs were obtained using a JSM-6330F field emission-scanning electron microscope (JEOL, Japan).

2.2. Synthesis of allobarbital

The synthesis and characterization of allobarbital were performed according to Ref. [26]. The results: mp: 173–174 °C; IR peak (KBr) (cm^{-1}): 3205, 3094, 2930, 2862, 1702; ^1H NMR ($CDCl_3$) (ppm): δ 7.96 (s, 2H), 5.58–5.68 (m, 2H), 5.15–5.22 (m, 4H), 2.74 (d, 4H, 7.6 Hz,); ^{13}C NMR (ppm): 42, 57, 121, 130, 148, 171.

2.3. Molecular simulation

The binding energy (ΔE) of the template molecule and the monomer was calculated using the density functional theory (DFT) [27] with Gaussian 03 software [28]. Firstly, the conformations of ABA, acrylamide (AAM), SMT, and the complexes of ABA and SMT, plus AAM and SMT were optimized under vacuum using the self-consistent reaction field (SCRF) methods at B3LYP/6-31G* level. All of the stable structures were further evaluated by analytical computations of harmonic vibrational frequencies. The energies of ABA, SMT, AAM–SMT, AAM–SMT–AAM, ABA–SMT and SMT–ABA–SMT were calculated with zero-point energy corrections. The ΔE of the complexes, such as AAM–SMT, AAM–SMT–AAM, ABA–SMT, DAHT–ABA and SMT–ABA–SMT, were calculated using Eq. (1), as follows:

$$\Delta E = E\,(\text{complex}) - E\,(\text{ABA or AAM}) - E\,(\text{SMT}) \quad (1)$$

Thus, a higher ΔE implies a stronger affinity between ABA, AAM and SMT; the dipole moments of cyanazine and SMT were calculated by the same method.

The vibrational frequencies of SMT, ABA, SMT–ABA, SMT–ABA–SMT were simulated and calculated using the SCRF method, in a chloroform medium at B3LYP/6-31G* level [29].

2.4. Preparation of SMT-MIMs

Precipitation polymerization appears to be one of the most attractive and reliable methods to obtain spherical particles with sufficient porosity, as reported previously [30]. Acetonitrile and toluene, with poor hydrogen bonding capacity, were used to prepare monodisperse microspheres with a uniform particle size and low swelling factor by thermal-induced free-radical polymerization [31]. We used the following synthesis procedure: the template (SMT, 1.8 mmol) and the functional monomer (ABA, 1.8 mmol), were added to a flat-bottomed flask. DVB (2.88 mL, 20 mmol), a mixture of toluene:acetonitrile (180 mL, 1:3, v/v), and AIBN (170 mg) were subsequently added. The resulting solution was degassed by ultrasound for 5 min and the flask was closed and sealed. The polymerization was accomplished in a water bath at 60 °C for 72 h. The non-imprinted microspheres (NIMs) were obtained following the same procedure in the absence of the SMT.

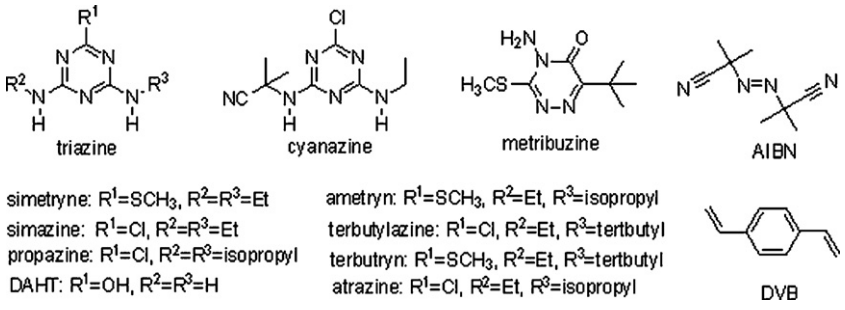

Fig. 2. The chemical structure of materials used in this study.

2.5. Infrared spectroscopy characterization

Infrared spectra of the liquid sample were measured in a temperature controlled NaCl solution phase cell with a 0.1 mm path length. The spectrum of particulate MIMs was obtained directly on a KBr plate. For the characterization experiments, the concentration of the host and guest molecules was 0.1 mol/L in $CHCl_3$. To investigate the differences in the IR spectra of the MIMs before and after absorbing SMT, the MIMs were soaked for 20 h in the solution of 10 mg/L SMT in $CHCl_3$ to rebind with SMT, and then characterized by IR.

2.6. Chromatographic evaluation of MIMs

1.8 g of dry MIMs was left to swell in methanol for 4 h, and then packed into stainless steel columns (150 mm × 4.6 mm id) under 40 MPa of air pressure. The columns were connected to a CBM-10Avp plus HPLC system equipped with a binary high-pressure pump, a manual sampler and a programmable UV detector. The residual template and monomer were completely eluted with a mobile-phase consisting of acetic acid: methanol (30:70, v/v) at 0.2 mL/min until a stable base line was obtained.

To optimize the chromatographic conditions, the flow rate, components of the mobile phase and column temperature were investigated in detail by injecting a given volume of the SMT standard solutions into the columns. The capacity factors (k) were calculated using the equation

$$k = \frac{t_R - t_0}{t_0}$$

where t_0 is the retention time of acetone (used as a void marker) and t_R is the retention time of the analyte. The imprinting factor (IF) was calculated from the capacity factors of the MIM and NIM columns using the equation

$$IF = \frac{k_M}{k_N}$$

2.7. Sample preparation

10 g of corn particles of 16–28 μm diameter was mixed with 40 mL of acetonitrile [21]. The corn mixture was sonicated for 30 min, and the supernatant was filtered through a 0.45 μm filter. The extract was evaporated to dryness in a rotary evaporator under reduced pressure, and dissolved in 3× 1 mL of acetonitrile. The resultant solution was collected in 5 mL plastic centrifugal tubes and dried under a gentle stream of nitrogen. The residue was re-dissolved in 1.0 mL of acetonitrile containing SMT for molecular imprinting solid phase extraction (MISPE).

10 g of soil, dried at room temperature and powdered to obtain 16–28 μm particles, was spiked with 1 mL of a standard solution of simazine with SMT. The soil samples were extracted using a Soxhlet extractor for 20 h, using 150 mL of acetonitrile. The extract was treated in a manner similar to the procedure used with corn samples, but re-dissolved in 1 mL of acetonitrile:water (50:50, v/v) mixture for MISPE. The contaminated and spiked soil samples were processed in the same way, except that the standard solution of triazine herbicides was not added to the contaminated samples.

2.8. MISPE of sample extracts

After removal of the template molecules, 0.2 g of SMT-MIMs was placed in an empty 3 mL SPE cartridge with two matched sieve plates placed above and below the sorbent bed. 10 mL of acetic acid: methanol (30:70, v/v) and 10× 1 mL of methanol were then successively applied to the cartridge in order to remove the residual acetic acid completely.

After a series of experiments to optimize the loading, washing and eluting conditions for corn and soil samples, the MISPE experiments were performed as follows. (i) The prepared MISPE cartridge was conditioned with 3.0 mL of methanol, followed by 9.0 mL of loading solvent (acetonitrile for corn sample and acetonitrile:water (50:50, v/v) for soil sample). (ii) 1 mL of sample solution was loaded onto the cartridge at a flow rate of 0.25 mL/min. Then the cartridge was washed with 1.0 mL of acetonitrile:water (50:50, v/v) in the case of the contaminated corn sample and 2.0 mL of acetonitrile:water (20:80, v/v) in the case of the soil sample. (iii) The analytes were eluted with 2× 1 mL of methanol, the combined elution solution was evaporated to dryness and re-dissolved in 1.0 mL of methanol:water (80:20, v/v) for corn sample and (60:40, v/v) for soil sample, for further HPLC analysis. All samples were prepared and analyzed in triplicate.

Table 1
Binding energies of the complexes of SMT and ABA (AAM).

Compound	Energy (a.u.)	Binding energy (a.u.)	Binding energy (kJ/mol)
ABA	−723.2545	–	–
SMT	−985.6438	–	–
AAM	−247.2188	–	–
ABA–SMT	−1708.9188	−0.0205	−53.8
AAM–SMT	−1232.8754	−0.0127	−33.4
SMT–ABA–SMT	−2694.5829	−0.0408	−107
AAM–SMT–AAM	−1480.1103	−0.0289	−75.8

3. Results and discussion

We have designed the SMT-MIMs with an amide as the functional monomer, basing our idea upon the example of the nucleic acids' base pairs. The binding energy values calculated from molecular simulations show that a cyclic amide can bind to SMT better than acrylamide, which gave us the idea to synthesize a cyclic amide (ABA) and prepare novel MIMs with the hydrogen bond array of "DAD (donor–acceptor–donor)–ADA (acceptor–donor–acceptor)". A molecular binding model was derived from the results obtained by molecular simulation and IR. The molecular recognition mechanism of MIMs was then investigated using the HPLC method. Finally, the MIMs were used in the extraction of SMT from corn and soil samples, and then detected by the HPLC.

3.1. Molecular simulation

A prerequisite for the creation of non-covalent MIMs is that the functional monomer should be able to form a stable complex with the template molecule during pre-polymerization. The stronger the interaction of the template with the functional monomer, the more stable the formed complex, and the better the molecular recognition capacity of the resulting MIP.

Many interesting studies have been carried out in which SMT-MIMs were prepared by bulk polymerization using MAA as the functional monomer. However, so far, there are no reports of triazine-MIPs having been prepared by using an amide to fulfill that function. This may be due to the non-covalent bond interactions between acrylamide and triazine herbicides being too weak. In the work presented here, we selected a cyclic amide and acrylamide (AAM) for SMT-MIM preparation, in order to study the molecular binding characteristics and recognition mechanism of SMT-MIMs with amide as a functional monomer.

The binding energy values of the host–guest system were calculated by molecular simulation with SMT as the template molecule, and AAM or ABA as the functional monomer (Table 1). SMT–ABA

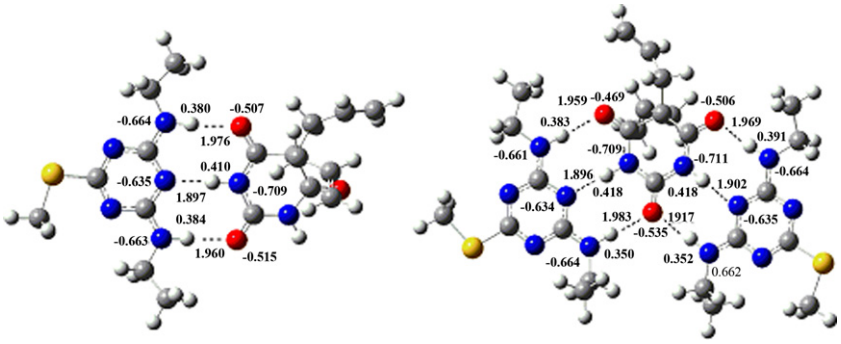

Fig. 3. Configurations of the interactions between the template molecule and monomer with different ratios: (a) ABA–SMT and (b) SMT–ABA–SMT. The numbers represent the corresponding atomic charges or hydrogen bond lengths.

and SMT–ABA–SMT can transform spontaneously to a hydrogen bond array configuration from any given initial state (Fig. 3). The binding energies of SMT–ABA and SMT–ABA–SMT were about 20 and 31 kJ/mol higher than those of AAM–SMT and AAM–SMT–AAM, respectively. We deduced that ABA and SMT form a three-point hydrogen bond array of "DAD–ADA" pattern. At the same time, the binding energy of SMT–ABA–SMT was almost twice than that of ABA–SMT, indicating that two molecules of SMT bind to each molecule of ABA with high affinity. Therefore, ABA was selected as the functional monomer for preparing the SMT-MIMs.

To confirm further the hypothesis of a hydrogen bond array, two vibrational modes asymmetric stretching vibration (*Vas*) and symmetric stretching vibration (*Vs*) were investigated by molecular simulation. The N–H stretching vibration of SMT in the complex was clearly shifted to a shorter wave range, and the N–H vibration of ABA was weakened because of the formation of the hydrogen bond array. The absorption peaks (*Vs*), 3365 cm^{-1} for ABA–SMT and 3368 cm^{-1} for SMT–ABA–SMT, were much stronger than the others in the vicinity (SI Table S1).

3.2. Infrared spectroscopy investigation

Intra- and intermolecular hydrogen-bonding interactions are often studied with vibrational spectroscopy [32]; in the present research this method was used to characterize the non-covalent interaction of the ABA–SMT complex.

The infrared spectra above 2600 cm^{-1} of MIMs, ABA and SMT molecules in $CHCl_3$ are shown in Fig. 4. Bands at 3384 and 3442 cm^{-1} can be attributed to the free NH-stretching vibrations of ABA and SMT, respectively [33]. In the pre-reaction solution (a mixture of ABA and SMT), the NH stretching vibration of ABA is typically shifted to a lower frequency (3346 cm^{-1}) due to the formation of hydrogen bonds (N–H···O) [34]. In present study, six (N–H···O) vibration frequencies of SMT–ABA and SMT–ABA–SMT are very approximate (SI Table S1), so there is only one band at 3346 cm^{-1} after forming a hydrogen bonds array. This is in accordance with the molecular simulation and confirms the existence of a hydrogen bond array in the ABA and SMT complex during pre-polymerization.

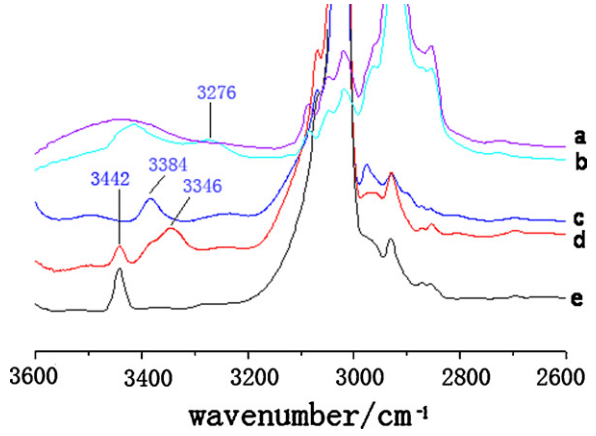

Fig. 4. Infrared spectra between 2600 and 3600 cm^{-1}: (a) MIMs before template rebinding; (b) MIMs after template rebinding; (c) ABA in $CHCl_3$; (d) a complex of ABA and SMT in $CHCl_3$; and (e) SMT in $CHCl_3$.

Our comparison of the IR spectra of the MIMs before and after rebinding template shows that the stretching vibration at 3276 cm^{-1} is due to the MIMs' rebinding template, which implies that the hydrogen bonds are formed as expected.

3.3. Nitrogen adsorption and SEM characteristics

The nitrogen adsorption of the SMT-MIM material is shown in Table 2. The MIMs have a regular spherical morphology and a larger specific surface area than the polymers synthesized by bulk polymerization, which could increase the opportunity for an interaction between SMT and the imprinted cavities. The MIM particle diameters are about 3–5 μm (SI, S7), which is favorable for HPLC stationary phase investigation of the MIMs' molecular recognition.

3.4. HPLC evaluation

Molecularly imprinted polymers are usually evaluated as the HPLC stationary phase because this method has good reproducibility, high efficiency and sensitivity. Thus, the MIMs produced in the present study were packed into the HPLC column to study their specific absorption capability and recognition mechanism.

In order to investigate the specific absorption, the columns of MIMs and NIMs were evaluated by eluting with different ratios of acetic acid (HAc):acetonitrile (v/v). The results showed that the capacity factors of SMT on both columns were reduced as the concentration of HAc was increased from 2% to 10% (Fig. 5). This could be attributed to the low concentration of HAc reducing the non-specific absorption of SMT on both MIM and NIM columns [35], and high concentration of HAc reducing non-specific absorption of MIMs and NIMs, further reducing specific absorption of MIMs. Therefore, the imprinting factor exhibited a maximum value (9.38) when the HAc content was 6%.

Table 2
Physical characteristics of the NIMs and MIMs.

Substance	S (m^2/g)	V_p (cm^3/g)	d_p (nm)
NIMs	568	0.30	2.14
MIMs	589	0.32	2.13

Note: BET specific surface area (S), specific pore volume (V_p) and average pore diameter (d_p) were calculated from nitrogen sorption measurements.

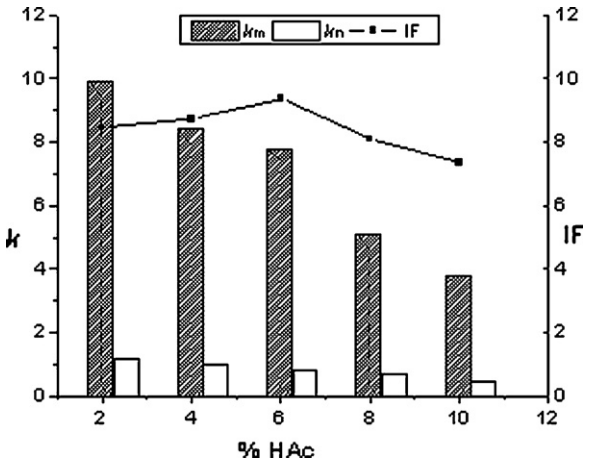

Fig. 5. The influence of HAc content in the mobile phase on the k_N, k_M and IF values. k_M and k_N are the capacity factors of the analytes in the MIM and NIM columns, respectively. HPLC conditions: detection, 254 nm; flow-rate, 0.6 mL/min; injected volume, 10 μL; marked peak, acetone.

To investigate the molecular recognition mechanism of MIMs, eight herbicides and a metabolite were applied as analogues of the template in this study. The capacity and selectivity factors of template and analogues on the MIM and NIM columns are shown in Table 3.

The results show an excellent retention of methylthio-triazines on the MIM column and the selectivity factors are good. The retention times of chloro-triazines on both the MIM and NIM columns were shorter than those of methylthio-triazines. It seems that the electron-withdrawing inductive effect of chlorine on the triazine cycle reduces the electron cloud density of the hydrogen bond array interaction. This hypothesis is consistent with the computer simulation results showing that the binding energies of SMT and simazine with monomer ABA are −53.76 and −52.90 kJ mol^{-1}, respectively.

The imprinting factor (9.38) for SMT was the highest among the methylthio-triazines, which indicates that the imprinting effect really occurs in SMT-MIMs and suggests that SMT-MIMs can selectively recognize the template molecule well via hydrogen bond array formation between the template and MIMs. The imprinting cavity of SMT did not completely match the bigger homologues ametryn and terbutryn, providing evidence of size-exclusion effects with molecular imprinting cavities [16]. The shortest retention time observed was for the metribuzin, a non-triazine herbicide, and was due to the lack of formation of a three-point hydrogen bond array between metribuzin and the MIMs.

We have carefully investigated the selectivity of MIMs and NIMs. A comparison has been made between MIM column and NIM column when the mobile phase was optimized for separating the mixture of triazine. But separating the mixture of triazine for NIM column was not made under optimization of HPLC conditions. Moreover, it is obviously observed from Table 3, the selectivity of MIMs is more superior than that of NIMs. Accordingly, we think that it is not necessary to further study the solid phase extraction of triazine mixture. Thus, we turn focus on the study of MIMs.

The retention times of triazine herbicides on both MIM and NIM columns increased with increasing alkyl group numbers. The hydrophobic property constant values (log *P*) are: SMT, 2.74; ametryn, 3.09; terbutryn, 3.65; simazine, 2.18; atriazine, 2.5; and terbutylazine, 3.21 [36,38]. It appears that the non-polar cross-linker DVB creates a hydrophobic backbone, providing additional nonspecific interactions between the methyl analogues and SMT-MIMs. In fact, the retention times of the methyl analogues on the MIM column were affected by both the stationary and mobile phases. However, the results still indicate that the hydrophobic interaction of alkyls and SMT-MIMs do not affect the imprinting factor because the large imprinting factor is caused by the pronounced retention of analytes on MIMs coupled with low retention on NIMs.

Both metabolite DAHT and cyanazine have the DAD (donator–acceptor–donator) configuration. According to computer simulation, the binding energy (−58.43 kJ mol^{-1}) of DAHT and ABA is higher than that of SMT and ABA (−53.76 kJ mol^{-1}), and the size of DAHT is smaller than that of the template molecule; thus the SMT imprinted cavity do not give a size-exclusion effect for DAHT. However, the short retention times and small imprinting factors of DAHT and cyanazine are possibly due to the mechanism of reversed-phase HPLC. There are no hydrophobic alkyl groups in DAHT, and cyanazine (calculated dipole moment: 7.75 D) is a more polar molecule than SMT (calculated dipole moment: 3.30 D). This greatly reduced the retention time on the hydrophobic MIM column.

In summary, it can be deduced that the recognition mechanism for the template and analogues is due mainly to a three-point hydrogen-bond array caused by electrostatic attraction and the electron effect of substitute groups in the triazine. The secondary interaction is provided by the imprinted cavity of the polymeric matrix, which possesses a steric (size and shape) and chemical (spatial arrangement of complementary functionality) memory for the template. The hydrophobicity and polarity of analytes also play a role in the retention times and imprinting factors on SMT-MIM column, especially while using hydrophobic DVB as a cross-linker.

Moreover, we obtained the complete baseline separation for five triazine analogues and a metabolite (DAHT) on SMT-MIM column at a flow rate of 0.6 mL/min, using methanol:water (95:5, v/v) as the mobile phase (Fig. 6). It can be seen in Fig. 6 that the SMT-MIM column exhibits good selectivity and presents attractive application prospects.

Table 3
Retention and selectivity factors of triazines in the MIM and NIM columns.

Solute	k_M[a]	k_N[a]	S[b]	γ[c]
Simazine	0.99	0.79	7.89	1.25
Atrazine	1.07	0.84	7.28	1.27
Terbutylazine	1.20	0.96	6.49	1.25
Propazine	1.13	0.95	6.89	1.19
Cyanazine	0.37	0.37	21.05	1.00
Simetryne	7.79	0.83	1.000	9.38
Ametryn	9.40	1.16	0.82	8.10
Terbutryn	11.40	1.38	0.68	8.26
Metribuzin	0.30	0.26	25.97	1.15
DAHT	1.06	0.82	7.35	1.29

The HPLC conditions were: eluent, acetic acid/acetonitrile (6/94, v/v); flow-rate, 0.6 mL/min; detection wavelength, 254 nm (to eliminate the effect of acetic acid); injection volume, 10 μL.

[a] k_M and k_N are the capacity factors of analytes on MIMs and NIMs, respectively.

[b] S is the selectivity factor ($S = k_{template}/k_{analogue}$), $k_{analogue}$ and $k_{template}$ are the capacity factor of template and analogues, respectively [36].

[c] γ is the imprinting factor ($\gamma = k_M/k_N$) [37].

3.5. MISPE-HPLC determination of triazines levels in corn and soil samples

We used corn and soil samples to evaluate the ability of the MIMs to recognize triazine herbicides in complex matrices. Corn was chosen because triazines are widely employed for its protection. The HPLC analysis was performed with eluent of methanol:water (80:20, v/v) for corn sample and (60:40, v/v) for soil sample, at a flow rate of 1.0 mL/min and detection at 230 nm. The injection volume was 20 μL.

The results from the MISPE-HPLC method showed good reproducibility for spiked corn sample. A good linearity was achieved

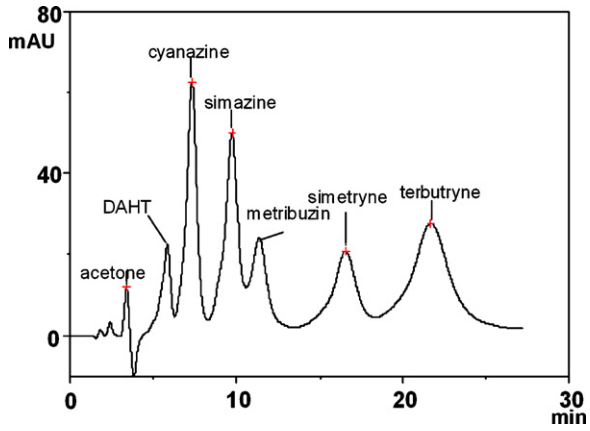

Fig. 6. Chromatograms (MIMs-HPLC) of five triazine herbicides and a metabolite (DAHT). HPLC conditions: detection wavelength, 230 nm; the concentrations of the five herbicides and DAHT were 20 μg/mL and approximately 5 μg/mL, respectively; marking peak: acetone.

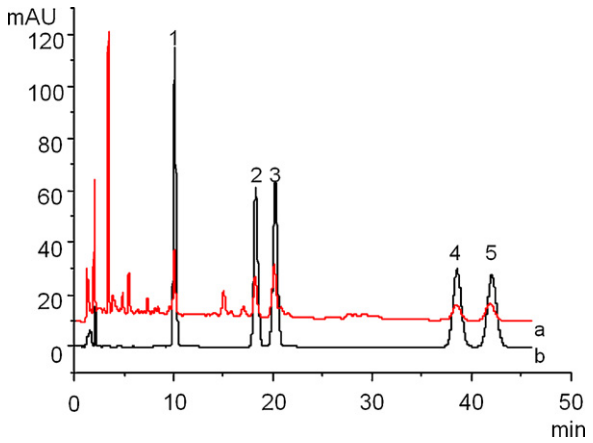

Fig. 8. Chromatograms obtained at 230 nm on the C18 column, (a) extract of a soil sample contaminated with 1.0 μg/mL of five triazines and (b) 10.0 μg/mL of triazines mixture standard solution. (1) Simazine, (2) simetryne, (3) atrazine, (4) ametryn, and (5) propazine. HPLC conditions: eluent, acetonitrile/water (30:70, v/v); flow rate, 1.0 mL/min; injection volume, 20 μL.

in the range of 0.2–0.8 μg/mL for simetryne, with correlation coefficient of 0.995. The interference peaks of impurities were decreased markedly after MISPE treatment. The recovery of SMT at the 0.20, 1.0 and 1.8 μg/mL concentration levels was 105% (R.S.D = 9.1%), 87.4% (R.S.D = 7.6%) and 90.7% (R.S.D = 1.0%), respectively. The detection limit was 5.8 μg/kg. Therefore, the MIMs can be applied in selective pretreatment and enrichment of low SMT levels in corn.

The simazine and SMT can be quantitatively detected in soil, even at low levels. Good reproducibility and a linear working range for both simazine and SMT were displayed from 0.01 to 0.20 μg/mL. The correlation coefficients of the calibration were >0.999 for both analytes. The recovery at 0.02, 0.1 and 0.2 μg/mL was 101% (R.S.D = 2.8%), 97.7% (R.S.D = 2.2%) and 94.6% (R.S.D = 2.0%) for SMT, and 107% (R.S.D = 4.6%), 93.6% (R.S.D = 8.7%) and 95.4% (R.S.D = 4.6%) for simazine. The detection limits of the MISPE-HPLC method were 0.075 μg/kg for simazine and 0.14 μg/kg for SMT, low enough to allow the environmental monitoring of triazines at realistic concentration levels.

In this study, the SMT-MIMs were employed for the simultaneous determination of simazine and SMT levels in real soil samples using the MISPE-HPLC system. In order to determine the amounts at the μg/kg level using a UV detector, 10 g aliquots of corn and soil powder were extracted and pre-concentrated with the MISPE. As shown in Fig. 7, the MISPE can completely eliminate the matrix interference in soil. The concentrations of simazine and SMT in the injection solution were determined to be 0.051 ± 0.003 and 0.138 ± 0.011 μg/mL according to corresponding regression equations, and their concentrations in soil were shown to be 5.1 ± 0.3 and 13.8 ± 1.1 μg/kg, respectively. The developed method in this wok showed comparable or even better results against reported method [21,39].

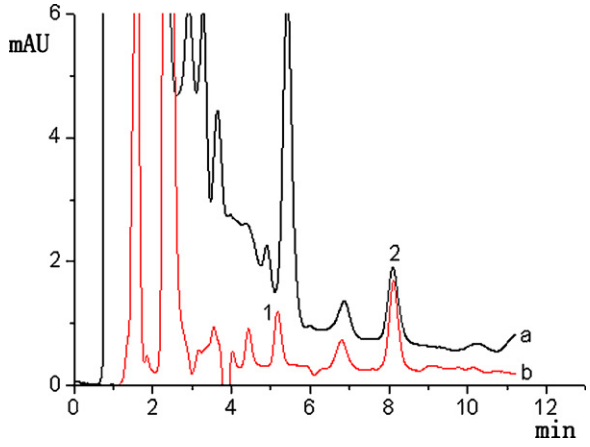

Fig. 7. HPLC chromatograms obtained at 230 nm on the C18 column, (a) extracts of soil sample without MISPE treatment and (b) extracts of soil sample with MISPE treatment. (1) Simazine and (2) simetryne.

To investigate further the competitive recognition and enrichment capacity of SMT-MIMs, the spiked soil samples were also prepared by adding 1.0 mL of a 1.0 μg/mL solution of five triazine herbicides (simazine, atrazine, propazine, SMT and ametryn) to 10 g of dry soil powder. After the MISPE treatment, five triazine herbicides were retained effectively (Fig. 8). This indicates that SMT-MIMs have good recognition capacity for triazine herbicides.

4. Conclusion

This study presents a set of methods for the elucidation of the molecular binding model and recognition mechanism of MIPs. The homogeneous host–guest binding sites originating from a three-point hydrogen bond array were characterized by molecular simulation and infrared spectroscopy. The molecule recognition mechanism of MIMs was studied with the SMT-MIMs as stationary phase in high performance liquid chromatography; five triazine herbicides and a metabolite were separated well on the SMT-MIM column. The high specific adsorption and excellent selectivity of MIMs can be attributed mainly to the hydrogen-bond array formed as the result of electrostatic attraction and the electron effect of substitute groups in the triazine. The secondary interaction is provided by the imprinted cavity of the polymeric matrix, which possesses a steric (size and shape) and chemical (spatial arrangement of complementary functionality) memory for the template. The hydrophobicity and polarity of analytes also have an impact on the SMT-MIM column's retention times and imprinting factors, especially when hydrophobic DVB is used as a cross-linker. The SMT-MIMs were also successfully applied in the selective pretreatment and enrichment of trace amounts of SMT in spiked corn and soil samples.

Acknowledgement

The National Natural Science Foundation of China supported this work (No. 20875034).

Appendix A. Supplementary data

Supplementary data associated with this article can be found, in the online version, at doi:10.1016/j.chroma.2011.01.008.

References

[1] G. Wulff, Angew. Chem. 107 (1995) 1958.
[2] J. Matsui, K. Fujiwara, S. Ugata, T. Takeuchi, J. Chromatogr. A 889 (2000) 25.
[3] X.G. Hu, Y.L. Hu, G.K. Li, J. Chromatogr. A 1147 (2007) 1.
[4] E. Gavioli, N.M. Maier, K. Haupt, K. Mosbach, W. Lindner, Anal. Chem. 77 (2005) 5009.
[5] N.A. O'Connor, D.A. Paisner, D. Huryn, K.J. Shea, J. Am. Chem. Soc. 129 (2007) 1680.
[6] B. Sellergren, Anal. Chem. 66 (1994) 1578.
[7] J. Matsui, K. Akamatsu, S. Nishiguchi, D. Miyoshi, H. Nawafune, K. Tamaki, N. Sugimoto, Anal. Chem. 76 (2004) 1310.
[8] K. Tappura, I.V. Lundin, W.M. Albers, Biosens. Bioelectron. 22 (2007) 912.
[9] G. Wulff, Chem. Rev. 102 (2002) 1.
[10] C. Alexander, C.R. Smith, M.J. Whitcombe, E.N. Vulfson, J. Am. Chem. Soc. 121 (1999) 6640.
[11] A.G. Strikovsky, D. Kasper, M. Grün, B.S. Green, J. Hradil, G. Wullf, J. Am. Chem. Soc. 122 (2000) 6295.
[12] D.J. Duffy, K. Das, S.L. Hsu, J. Penelle, V.M. Rotello, H.D. Stidham, J. Am. Chem. Soc. 124 (2002) 8290.
[13] Y. Kazuyoshi, T. Koichiro, T. Takeuchi, Anal. Chim. Acta 363 (1998) 111.
[14] K. Akimitsu, M. Takasi, T. Takeuchi, Analyst 26 (2001) 772.
[15] K. Hiroyuki, N. Hiroyuki, T. Takeuchi, Chem. Commun. 22 (2003) 2792.
[16] M. Panagiotis, A.J. Hall, C. Julien, Angew. Chem. 117 (2005) 3970.
[17] E. Tureil, A.M. Esteban, P. Fernández, C.P. Conde, C. Cámara, Anal. Chem. 73 (2001) 5133.
[18] F. Chapuis, V. Pichon, F. Lanza, S. Sellergren, M.C. Hennion, J. Chromatogr. A 999 (2003) 23.
[19] Y. Zhang, R.J. Liu, Y.L. Hu, G.K. Li, Anal. Chem. 81 (2009) 967.
[20] C. Cacho, E. Turiel, A.M. Esteban, C.P. Conde, C. Cámara, J. Chromatogr. B 802 (2004) 347.
[21] C. Cacho, E. Turiel, A.M. Esteban, D. Ayala, C.P. Conde, J. Chromatogr. A 1114 (2006) 255.
[22] I. Ferrer, F. Lanza, A. Tolokan, V. Horvath, B. Sellergren, G. Horvai, D. Barcelo, Anal. Chem. 72 (2000) 3934.
[23] R. Koeber, C. Fleischer, F. Lanza, K.S. Boos, B. Sellergren, D. Barcelo, Anal. Chem. 73 (2001) 2437.
[24] D. Djozan, B. Ebrahimi, Anal. Chim. Acta 616 (2008) 152.
[25] G. Wulff, B.O. Chong, U. Kolb, Angew. Chem. Int. Ed. 45 (2006) 2955.
[26] S. Kotha, A.C. Deb, R.V. Kumar, Bioorg. Med. Chem. Lett. 15 (2005) 1039.
[27] A.D. Becke, J. Chem. Phys. 98 (1993) 5648.
[28] M.J. Frisch, et al., Gaussian 03, Gaussian Inc., Pittsburgh, PA, 2003.
[29] S. Miertus, E. Scrocco, Tomasi, J. Chem. Phys. 55 (1981) 117.
[30] F.G. Tamayo, J.L. Casillas, A.M. Esteban, J. Chromatogr. A 1069 (2005) 173.
[31] J.F. Wang, P.A.G. Cormack, D.C. Sherrington, E. Khoshdel, Angew. Chem. Int. Ed. 42 (2003) 5336.
[32] K. Nakamoto, M. Margoshes, R.E. Rundle, J. Am. Chem. Soc. 77 (1955) 6480.
[33] J.S. Nowick, Q. Feng, T. Tjivikua, P.R.J. Ballester Jr., J. Am. Chem. Soc. 113 (1991) 8831.
[34] R. Buchet, C. Sandorfy, J. Phys. Chem. 88 (1984) 3274.
[35] R. Shoji, T. Takeuchi, I. Kubo, Anal. Chem. 75 (2003) 4882.
[36] S.T. Wei, B. Mizaikoff, J. Sep. Sci. 30 (2007) 1794.
[37] H. Sambe, K. Hoshina, J. Haginaka, J. Chromatogr. A 1152 (2007) 130.
[38] R.C. Martínez, E.R. Gonzalo, E.H. Hernández, Anal. Chim. Acta 559 (2006) 186.
[39] L. Chimuka, M. van Pinxteren, J. Billing, E. Yilmaz, J. Åke Jönsson, J. Chromatogr. A 1218 (2011) 674.